

Tissue-specific effects of saposin A and saposin B on glycosphingolipid degradation in mutant mice

Ying Sun^{1,4}, Matt Zamzow¹, Huimin Ran¹, Wujuan Zhang², Brian Quinn¹, Sonya Barnes¹, David P. Witte^{2,4}, Kenneth D.R. Setchell^{2,4}, Michael T. Williams^{3,4}, Charles V. Vorhees^{3,4} and Gregory A. Grabowski^{1,4}

From: ¹The Division of Human Genetics, ²The Division of Pathology and Laboratory Medicine and ³The Division of Neurology, Cincinnati Children's Hospital Medical Center and ⁴The Department of Pediatrics, University of Cincinnati College of Medicine, Cincinnati, OH 45229-3039.

Supplemental Figure Legends

Figure S1. Knock-in mutations on saposin A and saposin B by homologous recombination. (A) Targeting construct. The mutation in saposin A and saposin B (Cys→Phe) located on exon 4 and exon 7, respectively. Individual saposin was encoded by the exons under dotted line. The mutation destroys one of three disulfide bridges on the saposin, which leads to deficiency of saposin A and saposin B protein. The neo gene was removed by recombination on loxP sites through cross breeding of saposin AB heterozygous and Zp3-Cre transgenic mice. B, BamH I; Bg, Bgl II; H, Hind III; E, EcoR I; P, Pvu II; C, Cla I; K, Kpn I; Xh, Xho I. *, mutation site. (B) Targeted ES cells were confirmed by Southern blot using 3'probe. The clones were digested by Dra I/Bgl II that generated 11.7 kb fragment for WT and 5.6 kb for recombinant allele. (C) The mutations were confirmed by direct sequencing of PCR product generated from recombinant ES clone. Non-targeted ES clone was used as WT control. (D) PCR genotyping of saposin AB mice after Cre recombination using primers B-F and B-R across loxP site. The PCR product from wild type was 200 bp, and from AB^{-/-} without neo was 307 bp.

Figure S2. Alcian blue staining on AB^{-/-} mice. (A) WT mouse spinal cord. (B) AB^{-/-} mouse spinal cord. (C) AB^{-/-} mouse brainstem. (D) WT mouse kidney. (E) AB^{-/-} mouse kidney. (F) AB^{-/-} mouse white matter of cerebellum. AB^{-/-} mice showed sulfatide (blue) storage in brain, spinal cord and kidney tubules.

Figure S3. Sulfatide species levels in 10-14 weeks group by LC/MS analysis. (Upper panels) Major Sulfatide species in brain is C18:0 and C24:1 for NFA sulfatide and C18:0, C22:0, C24:1 and C24:0 for HFA sulfatide. C18:0 and C20:0 NFA and HFA sulfatides were accumulated in B^{-/-} and AB^{-/-} brain. (Middle panels) Long acyl chain HFA sulfatides (C20:0, C22:0, C24:0) were major species accumulated in B^{-/-} and AB^{-/-} mice kidneys. (Bottom panels) Accumulated sulfatide species in AB^{-/-} mice livers included both short and long acyl chain (C16:0 to C24:0). A^{-/-} and B^{-/-} mice in 10-14 weeks group were at terminal stage. The ages of mice in 10-14

weeks group are: A^{-/-} mice, 10-13 weeks; B^{-/-} mice, 14 weeks, AB^{-/-} mice, 12-14 weeks; and WT mice, 14 weeks. The amount of sulfatides were normalized by mg tissue weight (n=3 mice).

Figure S4. GalCer species levels in 10-14 weeks group by LC/MS analysis. In comparison to A^{-/-} mice, AB^{-/-} mice had decreased GalCer level in the brain and kidney. Major accumulated GalCer species were C24:1 and C18:0 in A^{-/-} mice brains, and C16:0, C20:0, C22 and C24:0 in A^{-/-} mice kidneys. GalCer was separated for GluCer by LC/MS analysis. Tissue samples are as described in Figure S3.

Figure S5. LacCer species levels in 10-14 weeks group by LC/MS analysis. Major accumulated LacCer species were C18:0 in the AB^{-/-} brain, C16:0, C18:0 and C24:0 in the A^{-/-}, B^{-/-} and AB^{-/-} kidney, and long acyl chain species (C22:0, C24:1 and C24:0) in the A^{-/-} and AB^{-/-} liver and spleen. Tissue samples are as described in Figure S3.

Figure S6. Lactosylceramide (LacCer) levels in liver by LC/MS analysis. Total LacCer levels increased with age in AB^{-/-} and A^{-/-} mice livers (n=3 mice).

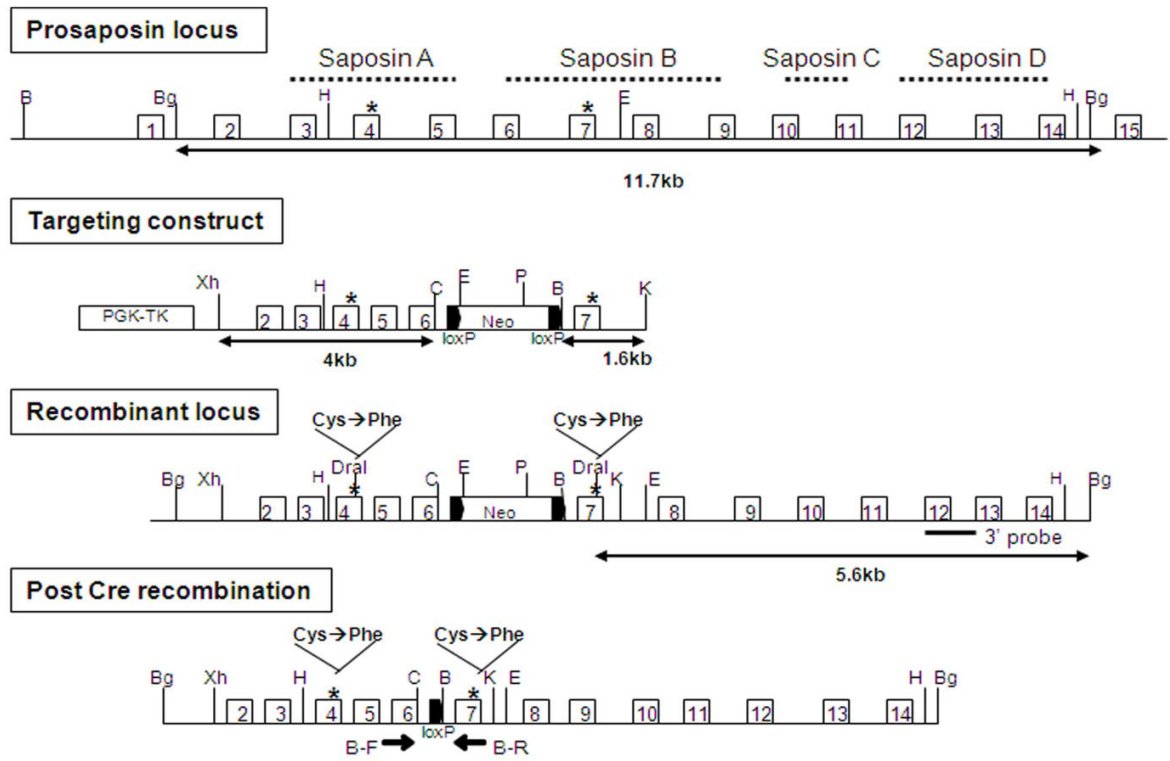
Figure S7. Glucosylceramide (GluCer) levels in 10-14 weeks group by LC/MS analysis. (A) Total GluCer levels were increased in AB^{-/-} mice brains and A^{-/-} and AB^{-/-} livers at 10-14 weeks of age. GluCer levels were differ between the A^{-/-} and the B^{-/-} and AB^{-/-} kidney, and not altered in the spleen of those mutant mice. Brain GluCer was separated from GalCer by LC/MS. (B) GluCer species. C18:0 is the dominant in the brain and C20:0 to 24:0 are the major GluCer species in the spleen and liver. GluCer was separated from GalCer by LC/MS analysis. Tissue samples are as described in Figure S3.

Figure S8. Ceramide levels in 10-14 weeks group by LC/MS analysis. (A) Total ceramide levels in A^{-/-} and AB^{-/-} mice brains were reduced compared to WT. A^{-/-} mice had significantly increased ceramide levels in the liver and spleen. Ceramide levels were not altered in the kidney of those mutants. (B) Ceramide species. C18:0 is major ceramide species in the brain. C16:0, C24:0 and C24:1 are the major species in kidney, liver and spleen. Tissue samples are as described in Figure S3.

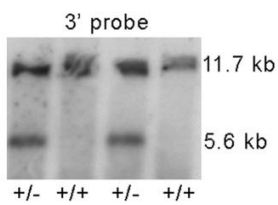
Figure S9. TLC analyses of GSLs. (A) Globotriaosylceramide (Gb3) levels were increased in AB^{-/-} liver and kidney. LacCer accumulation was in AB^{-/-} mice livers and sulfatide was enhanced in AB^{-/-} mice kidneys (n=2 mice). (B) Gangliosides in AB^{-/-} mice brains were at same levels as that in the WT mice. WT and AB^{-/-} mice samples were from 14 weeks old mice (n=3 mice).

Figure S1

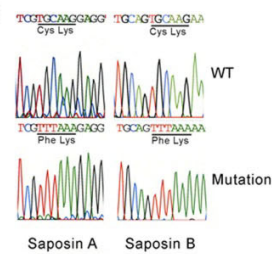
A



B



C



D PCR genotyping

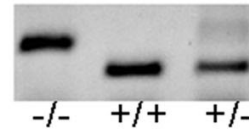


Figure S2

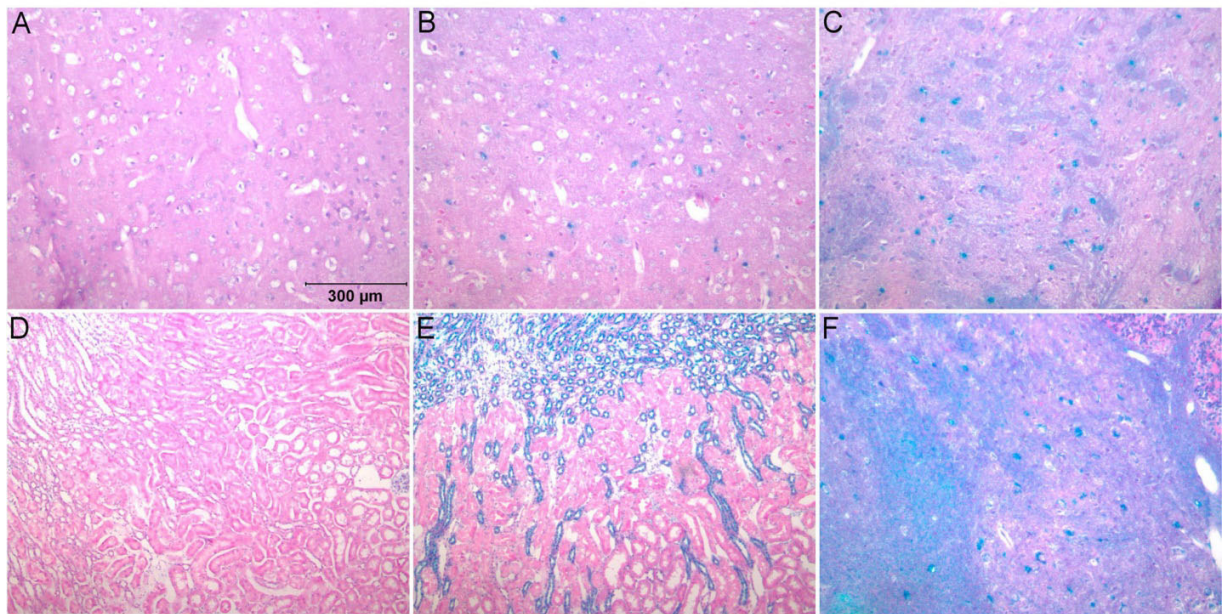
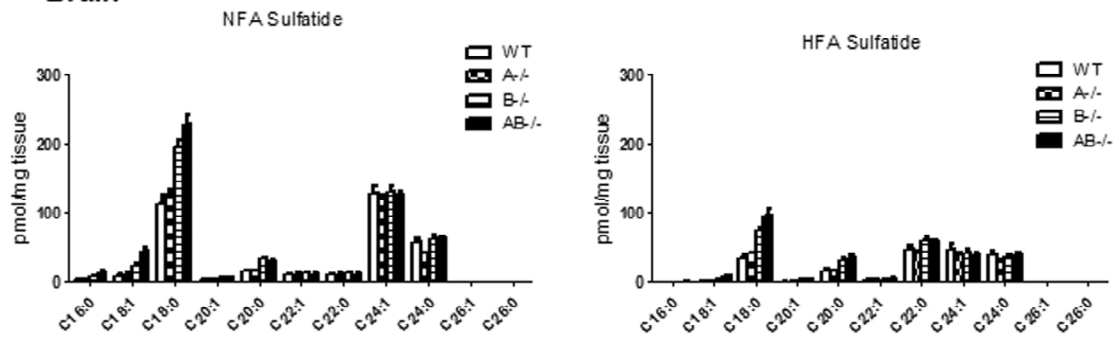
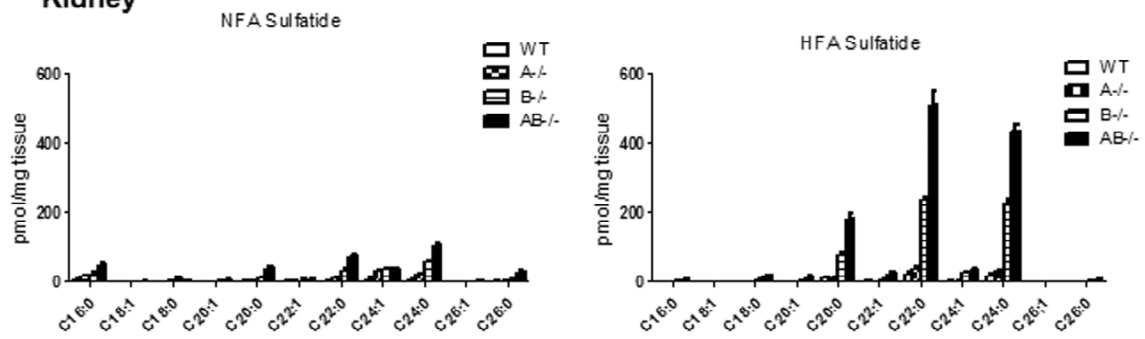


Figure S3

Brain



Kidney



Liver

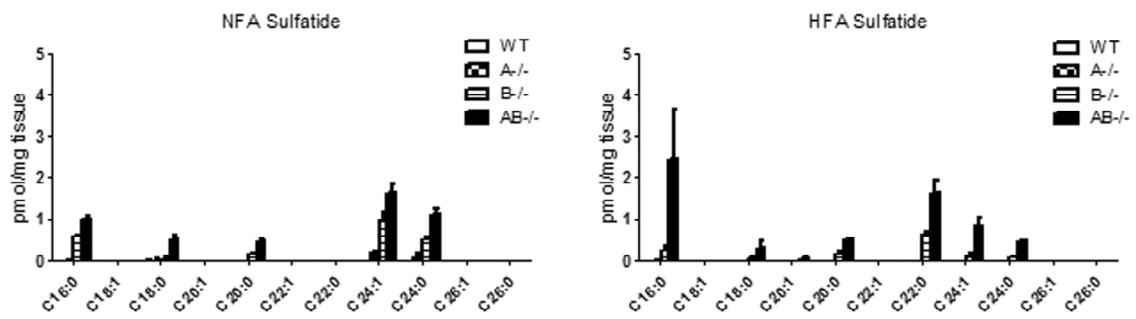
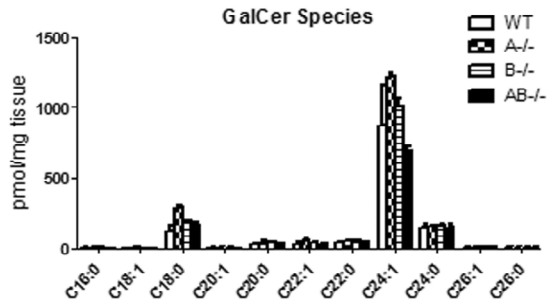


Figure S4

Brain



Kidney

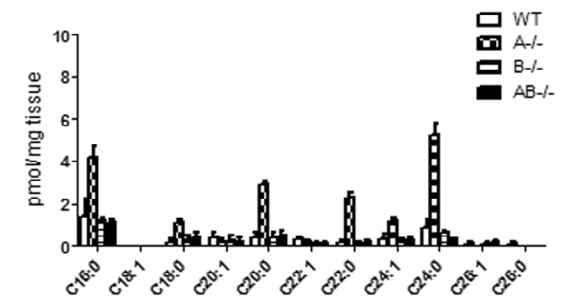
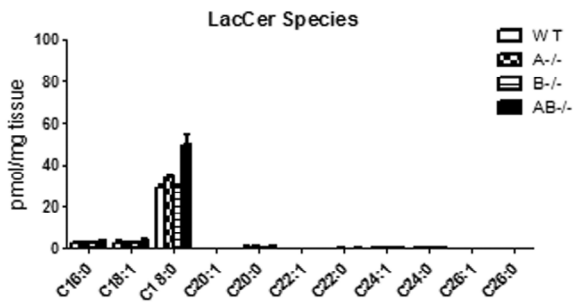
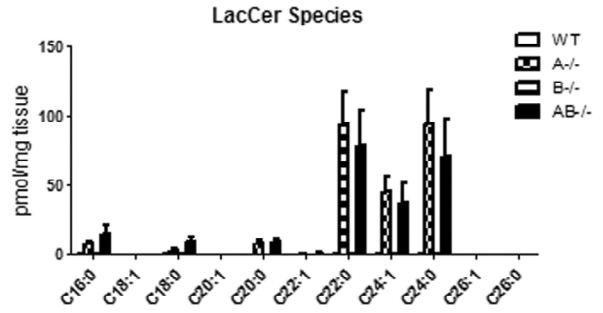


Figure S5

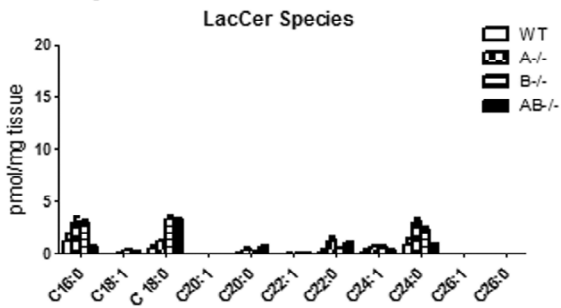
Brain



Liver



Kidney



Spleen

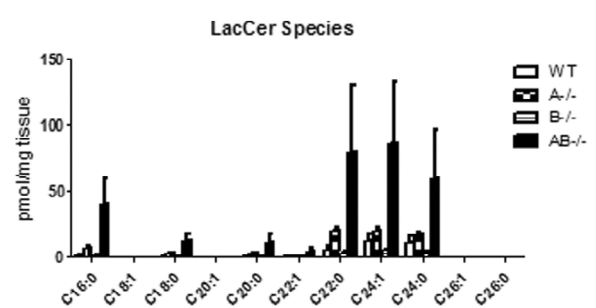


Figure S6

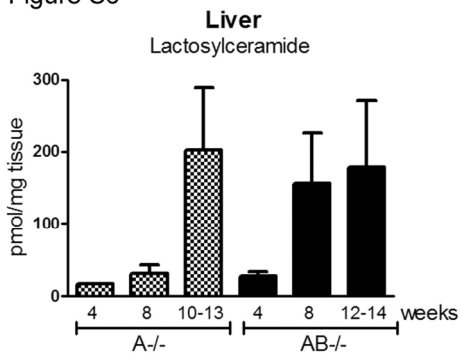
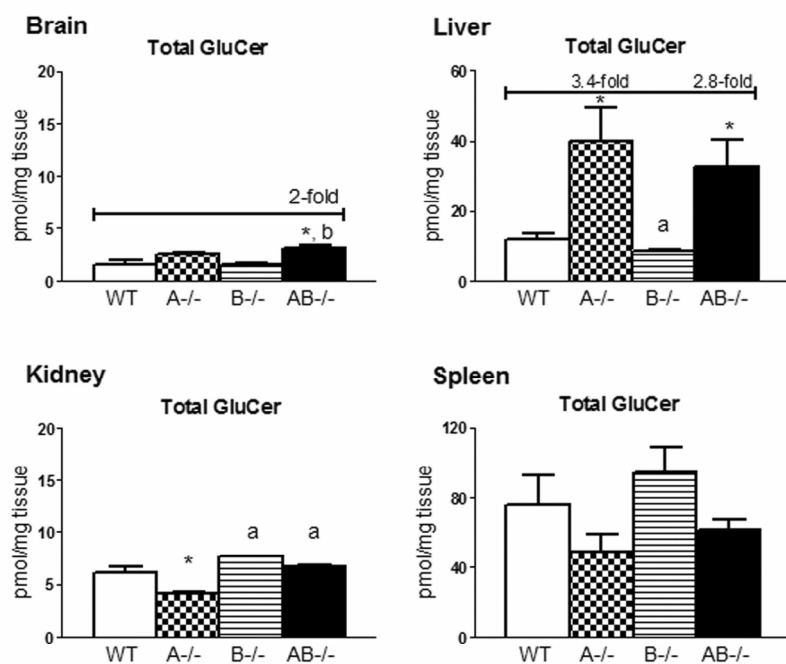


Figure S7

A



B

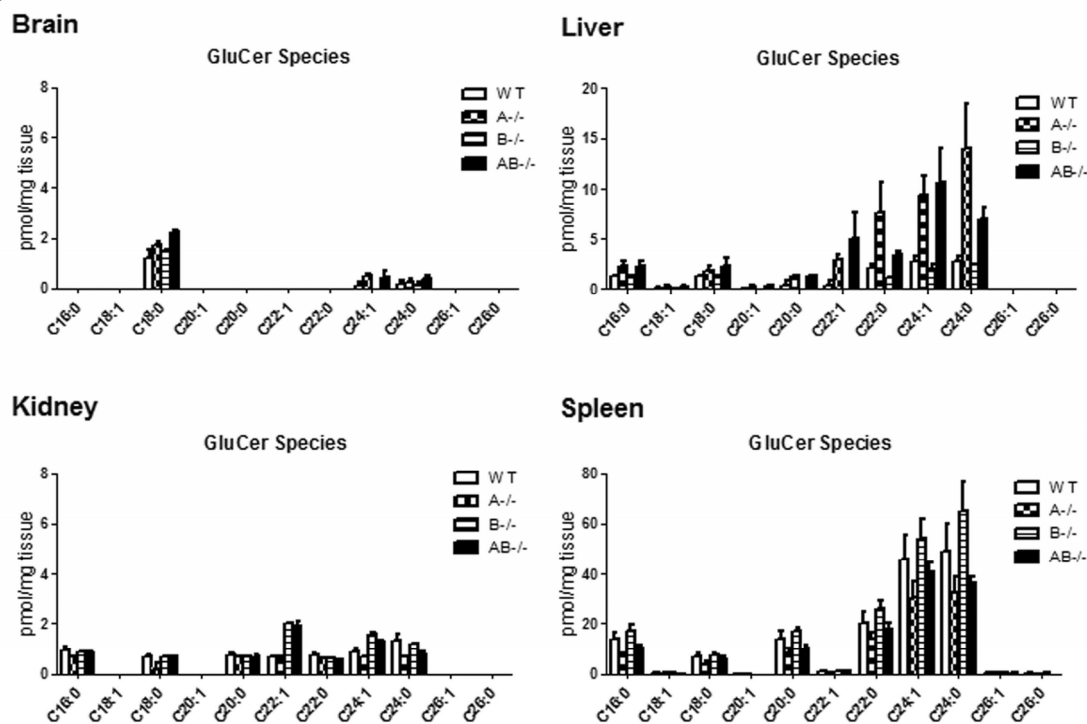
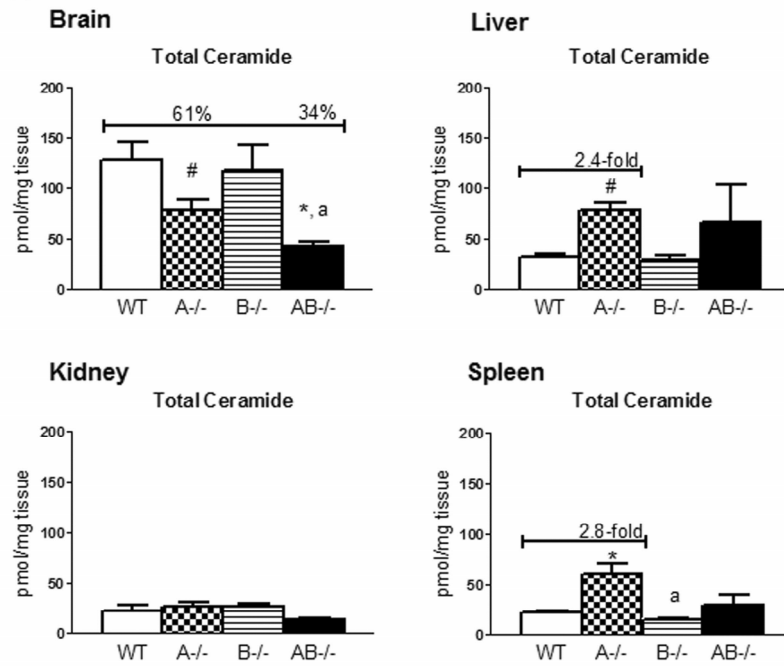


Figure S8

A



B

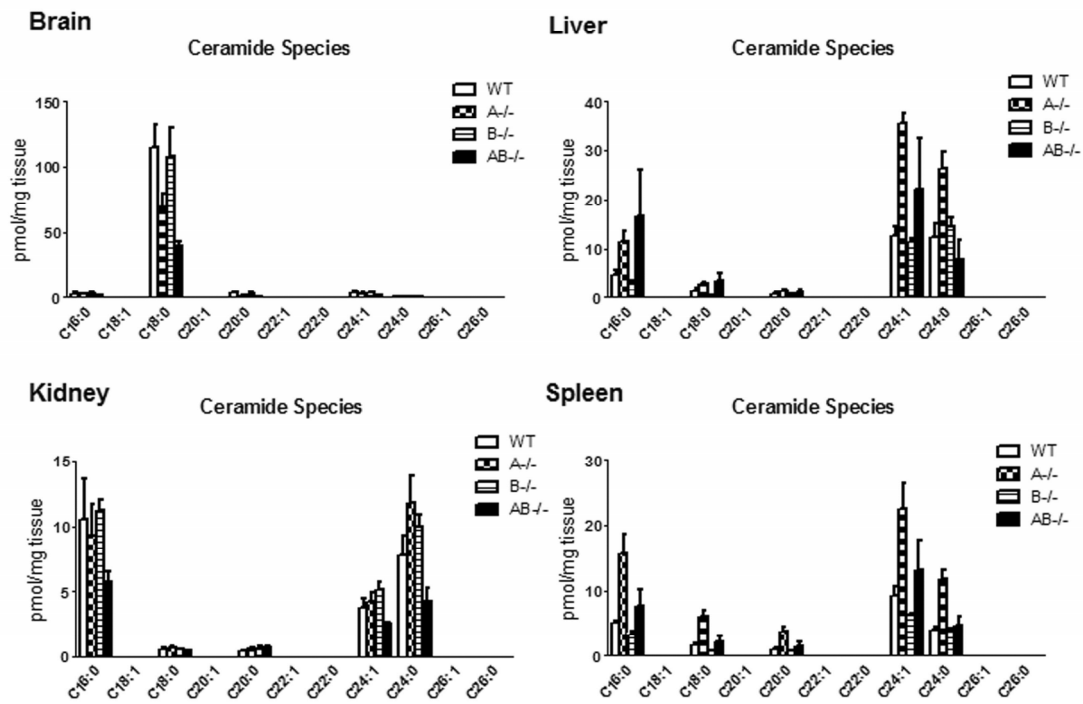
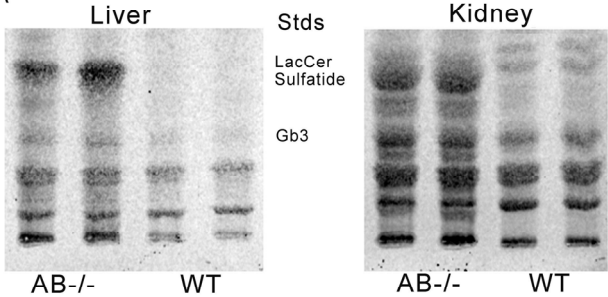


Figure S9

A



B

